Acta Crystallographica Section B
Structural Science
ISSN 0108-7681

Structural characterization of *p*-benzosemiquinone radical in a solid state: the radical stabilization by a low-barrier hydrogen bond

Krešimir Molčanov,[a] Biserka Kojić-Prodić[a]* and Mario Roboz[b]

[a]Rudjer Bošković Institute, POB 180, HR-10002, Zagreb, Croatia, and [b]Faculty of Food Technology and Biotechnology, University of Zagreb, Pierottijeva 6, HR-10000, Zagreb, Croatia

Correspondence e-mail: kojic@irb.hr

Received 27 December 2005
Accepted 22 September 2006

Semiquinone (*p*-benzosemiquinone), a transient organic radical, was detected in the solid state by EPR spectroscopy revealing four symmetrically equivalent protons. A variable-temperature X-ray diffraction analysis (293 and 90 K) and EPR data support a dynamical disorder of the proton. A low-barrier O—H···O hydrogen bond stabilizes the radical. The C—O bond length is 1.297 (4) Å, corresponding to a bond order of *ca* 1.5. The geometry of the radical implies an electron delocalization throughout the benzenoid ring. Two polymorphs of semiquinone, monoclinic and triclinic, were observed and their structures determined. Their crystal packings were compared with those of quinhydrone polymorphs.

1. Introduction

Quinones and their reduced forms, semiquinones and dihydroquinones (commonly named hydroquinones) occur in living systems as antioxidants and redox couples for electron-transfer reactions. The wide range of activities is related to quinone electronic characteristics with redox potentials ranging from +0.9 to +0.1 V. For 1,4-benzoquinone the redox potential is +0.715 V, which can be altered by changing the attached functional groups (to donate or withdraw electrons). The quinone ability for reversible oxidation and reduction (Fig. 1) plays an important role in a number of essential bioenergetic processes such as respiration and photosythesis. Coenzyme Q, the ubiquinone, exists in animals, plants and microorganisms; it is involved in electron transfer in photosynthesis (plastoquinones in photosystem II), oxidative phosphorylation, the bioactivity of vitamin K (phylloquinone in menaquinone), known as antihemorrhage vitamin, and others. There is a number of protein structures with various quinones bound to their reaction centres (Protein Data Bank, version November 2005; Berman *et al.*, 2000) either as substrates or as prosthetic groups. For example, NAD(P)H: quinone oxidoreductases, which catalyse two-electron reductions of quinones, have been intensively studied (Li *et al.*, 1995; Faig *et al.*, 2000). To the best of our knowledge, the only known example of a protein crystal structure which contains semiquinone is the photosynthetic centre of *Rhodobacter sphaeroides* (Stowell *et al.*, 1997). The structure of a complex of mutant S35C flavodoxin from a bacterium *Desulfovibrio vulgaris* with an isoalloxazine (*m*-semiquinone) radical has recently been reported (Artali *et al.*, 2005). Details on the geometry of the active sites revealed by the X-ray structure analysis of the quinone–protein complex depend very much on the resolution of the data collected. However, this experimental method cannot give the dynamics of the system and intermediates cannot be recorded. Reasonable resolution

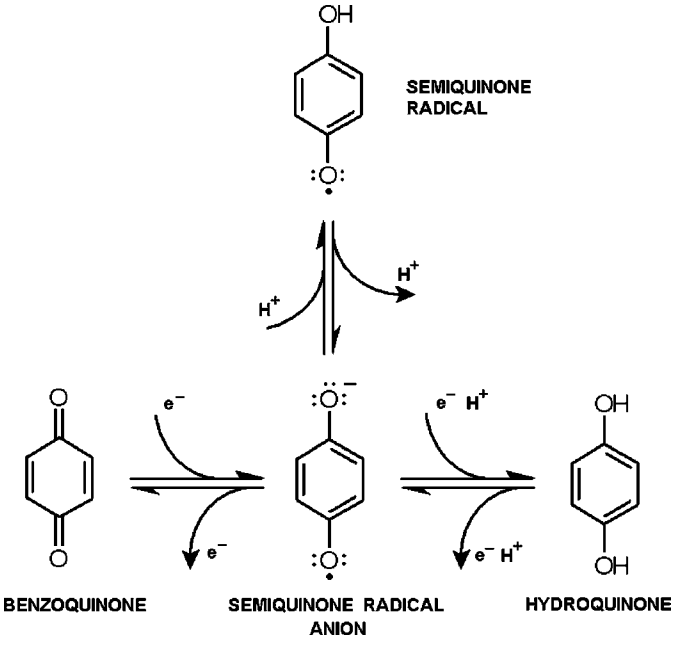

Figure 1
The proposed mechanism of the redox reaction benzoquinone/hydroquinone.

data of a protein complex and more accurate data obtained from small-molecule crystallography can be a good starting point for NMR and EPR spectroscopies to study the dynamics of the systems discussed (Guo *et al.*, 2002; Kolling *et al.*, 2003) and FTIR spectroscopy (Breton & Nabedryk, 1996; Mezzeti & Leibl, 2005). The redox properties of quinones are related to their chemical composition, but their interactions with protein at specific binding sites are influenced by the electronic properties of the groups involved, *in situ*. In redox processes of the quinones (Fig. 1) a radical intermediate, semiquinone, is formed. Semiquinone can exist as a protonated (neutral radical) or a deprotonated (radical anion) species (Fig. 1). Semiquinone is a paramagnetic species and its reactions can be studied by EPR spectroscopy. This method gives an insight into interactions of the radical and protein and/or solvent molecules (Guo *et al.*, 2002; Kolling *et al.*, 2003; Dikanov *et al.*, 2004). The new developments in high-field EPR methods provide information on the anisotropy of the *g* electronic tensor of bioradicals, such as semiquinone, and the probing interactions occurring between a protein and the radical. The theoretical approach based on density-functional theory (DFT) gives a calculated value for the electronic *g* tensor of a particular radical in an isotropic environment and in protein complexes of various photosynthetic reaction centres which can be compared with EPR experimental values (Kaupp, 2002; Ciofini *et al.*, 2004). To obtain a more realistic view of the biological system a static X-ray model is not sufficient, but its reliable data can be used as the inital parameters for theoretical calculations in the optimization of chemical structures to be compared with spectroscopic data.

In the present work we report on the simplest among the semiquinone radicals, *p*-benzosemiquinone, in the solid state as studied by EPR spectroscopy and structural characterization of its monoclinic and triclinic polymorphs by X-ray analysis. The crucial differences between the structures of *p*-benzosemiquinone and quinhydrone are illustrated in Figs. 2(*a*) and (*b*). In the solid state quinhydrone is a stable system where alternated benzoquinone and hydroquinone molecules are linked together by hydrogen bonds (brownish-green crystals of m.p. 444 K). The first X-ray study of quinhydrone was performed by Foz and Palacios in 1932 (Foz & Palacios, 1932). They observed the monoclinic space group $P2_1/n$ with cell parameters $a = 3.85$, $b = 6.04$, $c = 10.90$ Å, $\beta = 90^\circ$. The cell they obtained can accomodate only two benzenoid rings; an asymmetric unit is half of a molecule. The authors proposed a semiquinone structure (Fig. 2*a*). Subsequent measurements (Palacios & Foz, 1935; 1936), however, revealed weak reflections between layers in the *a* and *c* directions, indicating that the *a* and *c* axes should be doubled (7.70 and 21.8 Å, respectively). A structure with separated benzoquinone and hydroquinone rings (quinhydrone-type, Fig. 2*b*) is more plausible. Measurements of a magnetic anisotropy (Banerjee, 1939) gave further support to the coexistence of benzoquinone and hydroquinone molecules (quinhydrone type) in the crystal. The more elaborate X-ray structure analysis performed by Matsuda *et al.* (1958) definitely ruled out the semiquinone structure. Monoclinic quinhydrone was further refined by Sakurai (1968), who also discovered its triclinic polymorph (Sakurai, 1965).

A proton exchange between benzoquinone and hydroquinone is known to occur in aqueous solution and a radical intermediate, *p*-benzosemiquinone, is formed (Eggins & Chambers, 1970). Cooperative proton and/or electron transfer can also be induced in crystals of quinhydrone by high pressure (Mitani *et al.*, 1988; Shigeta *et al.*, 2001; Uchida *et al.*, 2002). An intermediate state of both electron- and proton-transfer processes, a semiquinone radical, can be stabilized at pressures of 1.5–3 GPa (Nakasuji *et al.*, 1991; Uchida *et al.*, 2002).

In this work emphasis is given to the proton transfer through a low barrier hydrogen bond which occurs in the crystal structure of semiquinone. The main step in the reduction of quinones (or, alternatively, oxydation of hydroquinones) is an electron transfer that is accompanied by a proton transfer (Fig. 1; Stowell *et al.*, 1997; Kolling *et al.*, 2003). As in many biochemical reactions, the proton transfer is

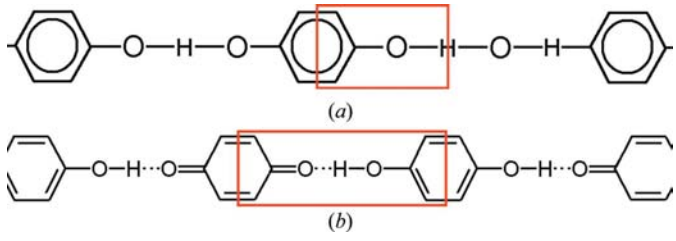

Figure 2
Hydrogen-bonded chains of (*a*) *p*-benzosemiquinone and (*b*) quinhydrone with highlighted asymmetric units in both structures.

through a low-barrier hydrogen bond (Cleland, 2000). Its potential energy is a double well (Fig. 3) with the energy barrier lower, or just slightly higher, than the zero-vibration level of a proton. The proton transfer takes place either by classic movement or by quantum-mechanical tunelling (Perrin & Nielson, 1997; Tuckerman *et al.*, 1997; Kumar *et al.*, 1998). The proton transfer along a low-barrier hydrogen bond is a ubiquitous phenomenon and the most important reaction in aqueous media (Tuckerman *et al.*, 1997; Gomez & Pacios, 2005).

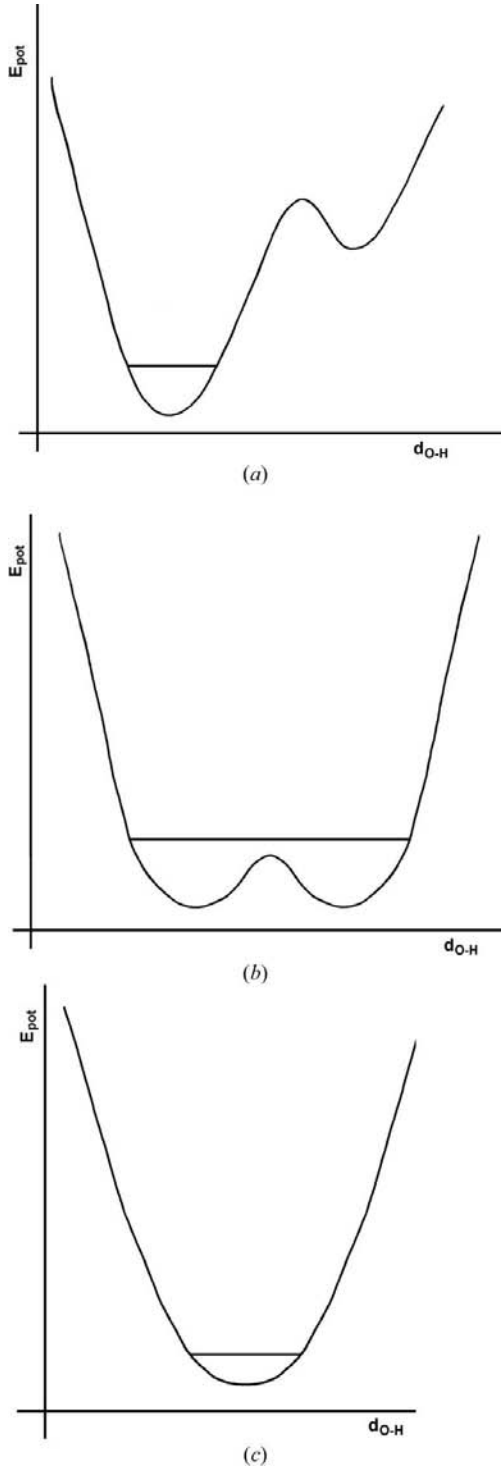

Figure 3
The potential energy wells of different types of hydrogen bonds: (*a*) double-well potential of a typical medium-strength hydrogen bond, (*b*) double-well potential of a low-barrier hydrogen bond in which the proton can move back and forth and (*c*) single-well potential of very strong, symmetrical, hydrogen bonds.

The molecular symmetry of *p*-benzosemiquinone and its resonance structures requires that a proton of the OH group be in dynamical disorder, accompanied by a low-barrier hydrogen bond. To characterize this type of hydrogen bond variable-temperature X-ray (VT-XRD) diffraction was used. Recently Wilson and coworkers (Parkin *et al.*, 2004; Wilson & Goeta, 2004; Nygren *et al.*, 2005) showed that this method is very efficient for describing a proton disorder. The variable-temperature neutron diffraction gives the average position of the proton (Wilson, 2001; Wilson *et al.*, 2001; Steiner *et al.*, 2001; Cowan *et al.*, 2003, 2005; Parkin *et al.*, 2004; Vishweshwar *et al.*, 2004), whereas VT-XRD gives the distribution of electron density along the hydrogen bond. Thus, the results of these two methods are complementary.

2. Experimental

2.1. Sample preparation and crystallization

Crystals of *p*-benzosemiquinone can be obtained from a mild alkaline aqueous solution of hydroquinone (Kemika; using a small amount of NaOH or a saturated solution of $FeSO_4 \cdot 7\,H_2O$). It is also possible to obtain *p*-benzosemiquinone by recrystallization of quinhydrone (Kemika) from protic solvents (water or ethanol). This method was employed to prepare *p*-benzosemiquinone crystals for the structure determination and recording EPR spectra. Single crystals of quinhydrone were obtained by recrystallization of quinhydrone (Kemika) from aprotic solvents (acetone or dimethylformamide; for measurements we used crystals precipitated from acetone solution). In order to be able to compare our crystallographic data with those obtained by Sakurai (1965, 1968), we followed his procedure to obtain quinhydrone by evaporation of acetone solution containing equimolar amounts of benzoquinone (Merck) and hydroquinone (Kemika).

2.2. Data collection and structure determination

All crystallographic measurements (if not stated otherwise) were performed on an Enraf–Nonius CAD-4 diffractometer (Cu $K\alpha$ radiation) equipped with an Oxford Cryosystems Cryostream 700 cooling device.

The transition between quinhydrone and semiquinone structures and the crystal structure of monoclinic quinhydrone at 100 K was measured on an Oxford Diffraction Excalibur 2 CCD diffractometer (Mo $K\alpha$ radiation) to verify the space-group symmetry of each species.

The *WinGX* program package (Farrugia, 1999) with implemented *SHELX*97 (Sheldrick, 1997) was used for structure solution, refinement and the calculation of difference-Fourier maps. The structures were refined by full-matrix least-squares against F^2 using all data. H atoms were located

Table 1
Crystallographic data of the triclinic (SQ_T) and the monoclinic (SQ_M) polymorph of *p*-benzosemiquinone.

	SQ_T90 K	SQ_M 293 K	SQ_M 90 K	SQ_T 293 K
Crystal data				
Chemical formula	$C_6H_5O_2$	$C_6H_5O_2$	$C_6H_5O_2$	$C_6H_5O_2$
M_r	109.1	109.1	109.1	109.1
Cell setting, space group	Triclinic, $P\bar{1}$	Monoclinic, $P12_1/c1$	Monoclinic, $P2_1/c$	Triclinic, $P\bar{1}$
Temperature (K)	90 (2)	293 (2)	90 (2)	293 (2)
a, b, c (Å)	3.7615 (6), 5.6996 (12), 5.9065 (8)	3.8362 (2), 5.9980 (3), 11.5007 (6)	3.770 (3), 5.980 (3), 11.458 (14)	3.8291 (2), 5.7546 (3), 5.9771 (2)
α, β, γ (°)	110.800 (15), 91.164 (12), 91.443 (15)	90, 108.7900 (10), 90	90, 109.99 (8), 90	111.121 (3), 89.936 (4), 92.453 (4)
V (Å^3)	118.28 (4)	250.52 (2)	242.8 (4)	122.73 (1)
Z	1	2	2	1
D_x (Mg m^{-3})	1.532	1.446	1.492	1.476
Radiation type	Cu $K\alpha$	Cu $K\alpha$	Cu $K\alpha$	Cu $K\alpha$
μ (mm^{-1})	0.97	0.92	0.95	0.94
Crystal form, colour	Rod, red	Plate, green	Plate, red	Rod, red
Crystal size (mm)	0.29 × 0.14 × 0.1	0.25 × 0.15 × 0.1	0.18 × 0.07 × 0.05	0.28 × 0.14 × 0.1
Data collection				
Diffractometer	Enraf–Nonius CAD4	Enraf–Nonius CAD4	Enraf–Nonius CAD4	Enraf–Nonius CAD4
Data collection method	Non-profiled $\omega/2\theta$ scans	Non-profiled $\omega/2\theta$ scans	Non-profiled $\omega/2\theta$ scans	Non-profiled $\omega/2\theta$ scans
Absorption correction	None	None	None	None
T_{min}	–	–	–	–
T_{max}	–	–	–	–
No. of measured, independent and observed reflections	1075, 499, 422	601, 523, 412	531, 507, 382	654, 513, 409
Criterion for observed reflections	$I > 2\sigma(I)$	$I > 2\sigma(I)$	$I > 2\sigma(I)$	$I > 2\sigma(I)$
R_{int}	0.056	0.066	0.102	0.062
θ_{max} (°)	76.4	76.0	75.8	76.2
No. and frequency of standard reflections	3 every 120 min	3 every 120 min	3 every 120 min	3 every 120 min
Intensity decay (%)	2	3	2	10
Refinement				
Refinement on	F^2	F^2	F^2	F^2
$R[F^2 > 2\sigma(F^2)]$, $wR(F^2)$, S	0.036, 0.106, 1.09	0.039, 0.106, 1.04	0.047, 0.131, 1.09	0.043, 0.124, 1.04
No. of reflections	499	523	507	513
No. of parameters	50	50	50	50
H-atom treatment	Refined independently	Refined independently	Refined independently	Refined independently
Weighting scheme	$w = 1/[\sigma^2(F_o^2) + (0.0482P)^2 + 0.0384P]$, where $P = (F_o^2 + 2F_c^2)/3$	$w = 1/[\sigma^2(F_o^2) + (0.0454P)^2 + 0.0735P]$, where $P = (F_o^2 + 2F_c^2)/3$	$w = 1/[\sigma^2(F_o^2) + (0.0849P)^2]$, where $P = (F_o^2 + 2F_c^2)/3$	$w = 1/[\sigma^2(F_o^2) + (0.0702P)^2 + 0.0343P]$, where $P = (F_o^2 + 2F_c^2)/3$
$(\Delta/\sigma)_{max}$	< 0.0001	< 0.0001	< 0.0001	< 0.0001
$\Delta\rho_{max}$, $\Delta\rho_{min}$ (e Å^{-3})	0.35, −0.2	0.22, −0.15	0.33, −0.42	0.24, −0.25
Extinction method	*SHELXL*	*SHELXL*	*SHELXL*	*SHELXL*
Extinction coefficient	0.054 (15)	0.025 (7)	0.053 (13)	0.06 (2)

Computer programs used: *CAD*4 *Express* (Enraf–Nonius, 1994), *XCAD*4 (Harms & Wocadlo, 1995), *SHELXS*97 (Sheldrick, 1997*a*), *SHELXL*97 (Sheldrick, 1997*b*), *ORTEP*3 *for Windows* (Farrugia, 1997, 1999), *WinGX publication routines* (Farrugia, 1999).

from difference-Fourier maps and no restraints were imposed upon their refinement. Owing to the small size of the crystals (Table 1[1]) and the fact that they contain only light atoms (O, C and H), no absorption correction was applied.

To study the role of hydrogen bonds on radical stabilization, intensity measurements of monoclinic semiquinone were performed at five different temperatures, from 90 K to room temperature. We will discuss only room-temperature and 90 K structures since the other three do not show any significant differences, but are of inferior quality ($R > 5\%$). A triclinic polymorph was measured at 90 K and room temperature. Difference Fourier maps were calculated using refined models (without H1) with data sets collected at various temperatures.

The crystallographic data and refinement details of the structures reported are given in Table 1.

2.3. EPR spectroscopy

EPR spectra were recorded by a Varian E-9 spectrometer using a frequency of 9.3 GHz. The compound α,α'-diphenyl-β-pycrylhydrazyl (DPPH) was used as an external standard [g_e = 2.0036 (3)]. The EPR spectrum, discussed in §§3.4 and 3.5, was recorded with a freshly precipitated crystalline sample, which was dried in air for *ca* 1 h. After 2 weeks the sample showed no

[1] Supplementary data for this paper are available from the IUCr electronic archives (Reference: WS5041). Services for accessing these data are described at the back of the journal.

EPR signal, indicating that the compound became diamagnetic over that period. The diamagnetic substance was identified as quinhydrone.

3. Results and discussion

The crystallization of quinhydrone was performed from aprotic solvents, whereas semiquinone was from protic ones. This finding suggests that the radical formation is *via* proton transfer (*i.e.* the formation of a *p*-benzosemiquinone radical anion) by a mechanism described by Eggins & Chambers (1970; Fig. 1). We discovered that the samples of semiquinone lost their paramagnetic properties after several days, whereas quinhydrone turns into semiquinone after exposure to X-rays. Apparently, the transition between these two structures is reversible and a single-crystal-to-single-crystal reaction occurred. Thus, semiquinone can be considered as an excited state of quinhydrone. Proton and electron transfer in quinhydrone crystals can be induced by high pressure or X-ray radiation under atmospheric pressure.

3.1. Transformation of quinhydrone to *p*-benzosemiquinone radical induced by X-rays

Data collection for both triclinic and monoclinic polymorphs of quinhydrone initially revealed unit cells of the quinhydrone (Sakurai, 1965, 1968). However, structure determination revealed a highly disordered model of very poor geometry. To understand the problem of disorder an analysis of the standard reflections (used for intensity control) was performed and non-systematic changes were observed. The analysis was extended to all measured reflections, observing that after *ca* 12 h some intensities of the reflections were reduced to below 30% of their initial values, whereas some retained 80% of their initial intensity values. There were also reflections that gained in intensity after an initial drop. X-ray oscillation images recorded by a CCD diffractiometer show this phenomenon clearly (Fig. 4). Non-systematic changes of intensities during the data collection of both polymorphs of quinhydrone suggest a chemical reaction in crystals induced by radiation. After exposure to X-rays for some time (*ca* 20–25 h), crystals initially identified as quinhydrone revealed semiquinone cells. The described non-systematic changes of intensities were observed for both monoclinic and triclinic polymorphs of quinhydrone.

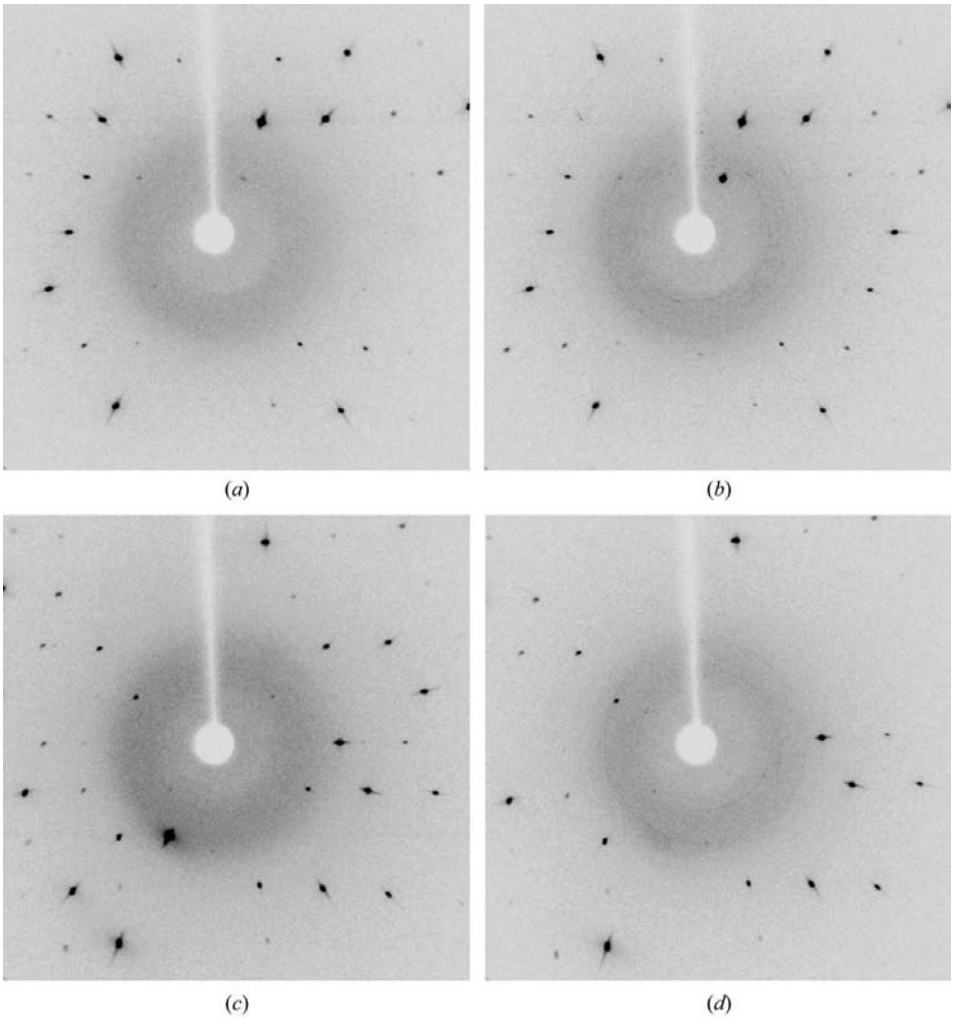

Figure 4
Oscillation X-ray images of triclinic quinhydrone in the directions of the *a* [(*a*) and (*b*)] and *c* axes [(*c*) and (*d*)] recorded by a CCD diffractometer prior to data collection [(*a*) and (*c*)] and after 20 h of exposure to X-rays [(*b*) and (*d*)].

However, the standard reflections of the monoclinic and triclinic polymorphs of semiquinone did not show any significant decay during data collection (*ca.* 12 *h*), but generally crystals were not very stable over a long exposure to X-rays (more than 20 h). The rate of transformation from quinhydrone to semiquinone and the amount of radiation absorbed by a crystal, before it deteriorates, depends on the size and quality of the crystal.

3.2. The relation of *p*-benzosemiquinone and quinhydrone unit cells and space groups

The unit cell of monoclinic *p*-benzosemiquinone is half the size of the unit cell of the monoclinic quinhydrone ($\mathbf{a}_{QH} = 2\mathbf{a}_{SQ}$). The unit-cell dimensions of both poly-

Table 2
Comparison of the unit-cell parameters of the monoclinic semiquinone (room-temperature data) and the monoclinic quinhydrone for both space groups, $P\,2_1/c$ and $P\,2_1/n$.

Compound	Space group	a (Å)	b (Å)	c (Å)	α (°)	β (°)	γ (°)
p-Benzosemiquinone[a]	$P2_1/n$	3.85	6.04	10.90	90	90	90
p-Benzosemiquinone[b]	$P2_1/c$	3.8362 (2)	5.9980 (3)	11.5007 (6)	90	108.790 (1)	90
p-Benzosemiquinone[b]	$P2_1/n$	3.8362 (2)	5.9980 (3)	10.8883 (6)	90	90.689 (4)	90
Quinhydrone[c]	$P2_1/c$	7.647 (1)	6.001 (1)	11.590 (1)	90	109.58 (3)	90
Quinhydrone[c]	$P2_1/n$	7.647 (1)	6.001 (1)	10.894 (1)	90	90.38 (3)	90
p-Benzosemiquinone[b]	$P\bar{1}$	3.7615 (6)	5.6996 (12)	5.9065 (8)	110.800 (15)	91.164 (12)	91.443 (15)
Quinhydrone[d]	$P\bar{1}$	7.652 (22)	5.956 (13)	6.770 (20)	107.61 (12)	121.93 (5)	90.28 (16)

References: (*a*) Foz & Palacios (1932); (*b*) this work; (*c*) Matsuda *et al.* (1958); (*d*) Sakurai (1965).

morphs of *p*-benzosemiquinone and quinhydrone were determined at room temperature for comparison with the values in the literature data (Foz & Palacios, 1932; Matsuda *et al.*, 1958, respectively; Table 2). To verify the unit cells and space groups of both compounds and their polymorphs measurements were taken at 100 K on a CCD diffractometer. The unit cells of *p*-benzosemiquinone (a = 3.84 Å) and quinhydrone (a = 7.65 Å) at low temperature are in agreement with previous measurements (Tables 1 and 2). The reflections of the smaller unit cell (*i.e.* *p*-benzosemiquinone), revealed systematic absences which are consistent with the space group $P\,2_1/c$ (Fig. 5*a*); determination of the crystal structure using these data resulted in reasonable accuracy (R = 0.055). In the $h0l$ layer of the semiquinone cell (Fig. 5*a*) reflections with l odd are systematically absent, as a result of the c glide plane. However, the reflections of the larger unit cell (corresponding to a monoclinic phase of quinhydrone) revealed systematic absences that are not in agreement with any space group, but can be understood as a result of the pseudosymmetry of a supercell (Fig. 5*b*). The transformation of the $P2_1/n$ cell (Foz & Palacios, 1932) led to the standard unit cell of the space group $P2_1/c$ reported in this work. Moreover, Matsuda *et al.* (1958) attempted to refine their structure as *p*-benzosemiquinone, however, they obtained a poorly refined structure (R = 0.24); structure determination with the quinhydrone model yielded reasonable agreement (R = 0.124). Our attempt to refine the structure of quinhydrone with the large cell using quinhydrone coordinates of Sakurai (1968) failed; the R factor could not be lowered below 0.45. Thus, the structure of Foz & Palacios (1932) should not be rejected as being incorrect because of crude instrumentation. Most probably, their experiment was performed by a crystal of *p*-benzosemiquinone in the monoclinic phase, while the subsequent experiments (Palacios & Foz, 1935, 1936; Banerjee, 1939; Matsuda *et al.*, 1958; Sakurai, 1968) dealt only with the monoclinic polymorph of quinhydrone.

3.3. Crystal packing

Crystal packings of the monoclinic polymorph of *p*-benzosemiquinone and the monoclinic polymorph of quinhydrone are similar (Fig. 6) with benzenoid rings having C_i symmetry.

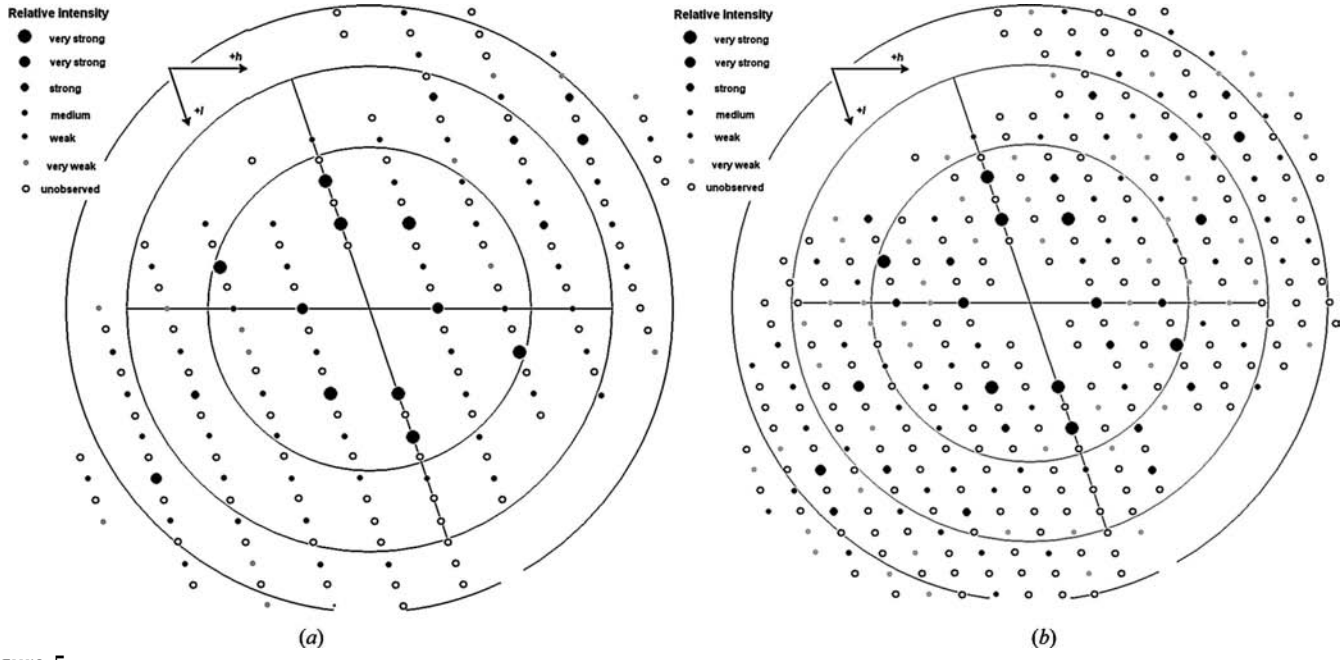

Figure 5
$h0l$ layers of reciprocal lattices: (*a*) monoclinic *p*-benzosemiquinone cell (a = 3.84 Å) and (*b*) monoclinic quinhydrone cell (a = 7.65 Å). Unobserved reflections are depicted as empty circles. The outer circle represents a resolution of 0.8 Å.

Table 3
Comparison of geometric parameters for the *p*-benzosemiquinone radical and its anion, and benzoquinone and hydroquinone molecules.

Compound	Method	C1—O1	C1—C2	C2-C3
p-Benzoquinone[a]	X-ray	1.222	1.469–1.479	1.330
Hydroquinone[b]	X-ray	1.379–1.381	1.378–1.393	1.383–1.392
p-Benzosemiquinone[c]	X-ray	1.297 (4)†	1.430 (5)†	1.359 (6)†
p-Benzosemiquinone anion × $2H_2O$[d]	DFT/B3LYP/EPR II	1.281	1.451	1.378
p-Benzosemiquinone anion × $4H_2O$[d]	DFT/B3LYP/EPR II	1.286	1.448	1.376
p-Benzosemiquinone anion[e]	DFT/BP86/DZP	1.267	1.461	1.383
p-Benzosemiquinone anion[e]	DFT/B3LYP/DZP	1.259	1.445	1.375
p-Benzosemiquinone anion[e]	DFT/BHLYP/DZP	1.246	1.443	1.364
p-Benzosemiquinone anion × $4H_2O$[e]	DFT/BP86/DZP	1.289	1.450	1.381
p-Benzosemiquinone anion[f]	Semiempirical/PM3	1.25 (1.26)‡	1.45 (1.45)‡	1.36 (1.36)‡
p-Benzosemiquinone anion[f]	DFT/B3LYP/ 6-31+G(d)	1.27 (1.28)‡	1.45 (1.44)‡	1.37 (1.37)‡
p-Benzosemiquinone anion[f]	DFT/B3LYP/EPR II	1.27 (1.29)‡	1.47 (1.45)‡	1.38 (1.38)‡
p-Benzosemiquinone anion[f]	DFT/B3LYP/EPR III	1.26 (1.28)‡	1.45 (1.44)‡	1.37 (1.37)‡
p-Benzosemiquinone anion[g]	DFT/B3LYP/ 3-21G*	1.284 (1.300)‡	1.453 (1.445)‡	1.369 (1.365)‡
p-Benzosemiquinone anion[g]	DFT/B3LYP/ 6-31G*	1.266 (1.277)‡	1.454 (1.448)‡	1.372 (1.371)‡
p-Benzosemiquinone anion[g]	DFT/B3LYP/ 6-31+G*	1.273 (1.278)‡	1.452 (1.448)‡	1.375 (1.374)‡
p-Benzosemiquinone anion[g]	DFT/B3LYP/ 6-31++G**	1.272	1.452	1.375
p-Benzosemiquinone anion[e]	DFT/BP86/DZP	1.288 (1.304)‡	1.461 (1.444)‡	1.380 (1.373)‡
p-Benzosemiquinone[h]	DFT/BP86/6-31G*	1.362 (1.264)§	1.422 (1.463)§	1.382
p-Benzosemiquinone[i]	DFT/B3LYP/ 6-31+G*	1.354 (1.256)§	1.413 (1.454)§	1.374

References: (*a*) Bolte & Lerner (2001); (*b*) Bolte *et al.* (2002); (*c*) this work; (*d*) Sinnecker *et al.* (2004); (*e*) Asher *et al.* (2004); (*f*) O'Malley (1997); (*g*) O'Malley & Collins (1996); (*h*) Nonella (1997); (*i*) Mohandas & Umapathy (1997). † Mean values for all structures reported in this paper with standard deviations in parentheses. ‡ Values for an isolated *p*-benzosemiquinone anion radical with values for a hydrogen-bonded one in parentheses. § Two symmetry-distinctive bonds are present; those at the deprotonated side of the molecule are in parentheses.

In the monoclinic semiquinone packing the hydrogen bonds are centrosymmetric with the H1 atom disordered over two symmetrically equivalent positions (site-occupancy factor, s.o.f. = 0.5) and details will be discussed in §3.5. The resulting molecular structure can be interpreted in two ways: statically disordered quinhydrone (a superposition of a benzoquinone and a hydroquinone molecule) or resonance structures of benzoquinone and hydroquinone (semiquinone radical) (Figs. 1 and 2). For a static disorder model the C—O bond should be a superposition of two bonds with respective lengths of 1.22 and 1.38 Å, and the atomic displacement ellipsoid of O1 should be significantly elongated along the C—O bond. However, the following experimental results are in favour of a dynamically disordered model (Figs. 1, 2 and 7). The values of the anisotropic displacement parameters of the atoms of the asymmetric unit do not show either high values or a pronounced anisotropy; the only exception is a slight elongation of the displacement parameter perpendicular to the C—O bond for the O1 atom (see anisotropic displacement parameters in supplementary data). Such ellipsoids indicate that neither static disorder nor tautomerism are present; the dominant motion of the O1 atom is wagging.

Crystal packing of the triclinic polymorph of *p*-benzosemiquinone was found to be similar to the crystal packing of the triclinic quinhydrone (Sakurai, 1965). The *p*-benzosemiquinone radical forms hydrogen-bonded chains composing a layered structure that is also observed in the crystal packing of quinhydrone (Fig. 8). There is no geometric transformation that could transpose the unit cell of triclinic quinhydrone to the unit cell of triclinic semiquinone. It is evident that triclinic *p*-benzosemiquinone and triclinic quinhydrone are two distinctive structures (Table 2, Fig. 8).

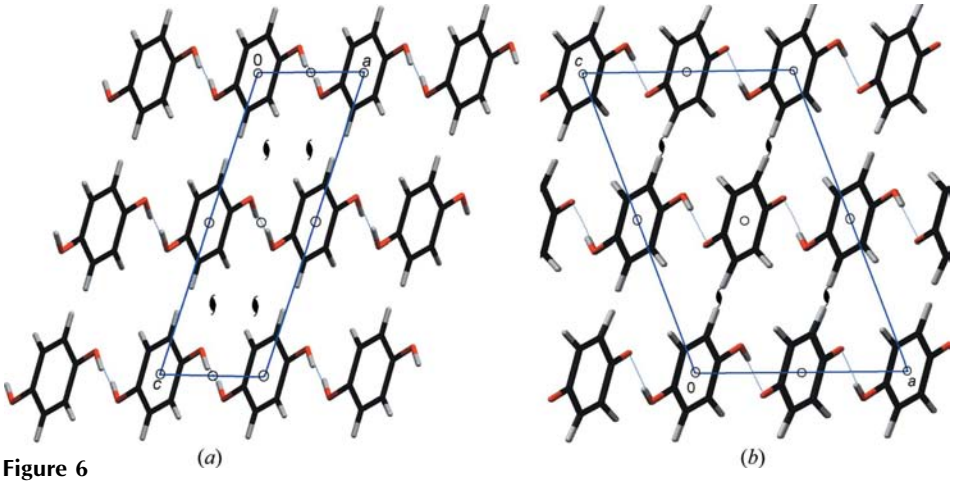

Figure 6
Crystal packing of (*a*) the monoclinic polymorph of *p*-benzosemiquinone and (*b*) the monoclinic polymorph of quinhydrone viewed normal to the *ac* plane with symmetry elements. In the monoclinic *p*-benzosemiquinone, the disordered H1 proton is drawn in symmetry-equivalent positions to emphasize the symmetry of the hydrogen bond, but each position is partly occupied by s.o.f. = 0.5.

3.4. Geometry of the *p*-benzosemiquinone radical

The *p*-benzosemiquinone radical can be viewed as a resonance hybrid (Fig. 7) of a centrosymmetric structure having an unpaired electron delocalized throughout the ring, as supported by quantum-mechanical calculations (O'Malley, 1997, 1998; Mattar *et al.*, 2002). In the crystal

structure the radical symmetry is C_i, where the centre of the benzenoid ring coincides with a crystallographic inversion centre. To obey the symmetry the H1 proton should be dynamically disordered. However, without the H1 proton the radical has a non-crystallographic symmetry (D_{2h}), which was predicted for the *p*-benzosemiquinone anion (O'Malley, 1997, 1998; Mattar *et al.*, 2002). The molecular geometry of the *p*-benzosemiquinone radical (Fig. 9) is between benzoquinone and hydroquinone with a C—O bond order of *ca* 1.5. This is in agreement with the known hybridization and conjugation effect (Table 3). bond length and angle differences, obtained from data collected at various temperatures, are within the limits of their standard deviations.

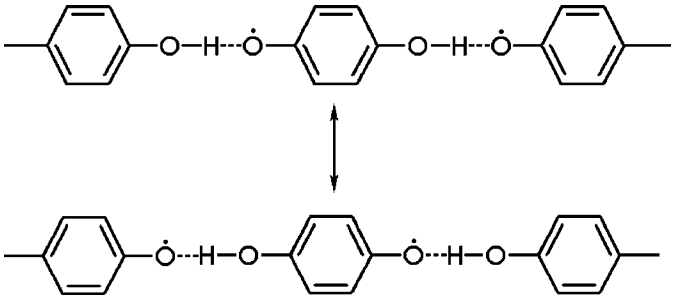

Figure 7
The two resonant structures of *p*-benzosemiquinone expected in crystals.

The geometric parameters of the *p*-benzosemiquinone radical anion obtained by quantum-mechanical calculations are listed in the Table 3 for comparison. They show significant variations; apparently the geometry very much depends on the method and basis set used for the calculations. The structures calculated are closer to benzoquinone than to hydroquinone (Table 3). They represent radical anions rather than neutral radicals. The hydrogen bond affects not only the C—O bond length, but also the geometry of the benzenoid ring. The geometry of the hydrogen-bonded *p*-benzosemiquinone anion radical is more similar to the *p*-benzosemiquinone radical stabilized by hydrogen bonds in the crystal than to the isolated (non-hydrogen bonded) species; thus, the results reported by Sinnecker *et al.* (2004), Asher *et al.* (2004, 2005) and O'Malley & Collins (1996) are in good agreement with the results of the X-ray structure analysis. However, DFT calculations for protonated (neutral) *p*-benzosemiquinone radicals (Mohandas & Umapathy, 1997; Nonella, 1997) predicted asymmetric molecules with the protonated side being more similar to hydroquinone (Table 3). Therefore, we conclude that the geometry of our radical is most similar to the calculated anion geometry and this is attributed to the H1 proton in dynamic disorder. This model is also supported by the solid-state EPR spectrum (Fig. 10), which shows four equivalent protons. Values g_e and a_o (2.0023 and 0.24 mT, respectively) agree well with those determined for *p*-benzosemiquinone anion radicals in aqueous solutions (Venkataraman & Fraenkel, 1955; Venkataraman *et al.*, 1959). The fifth proton, which is

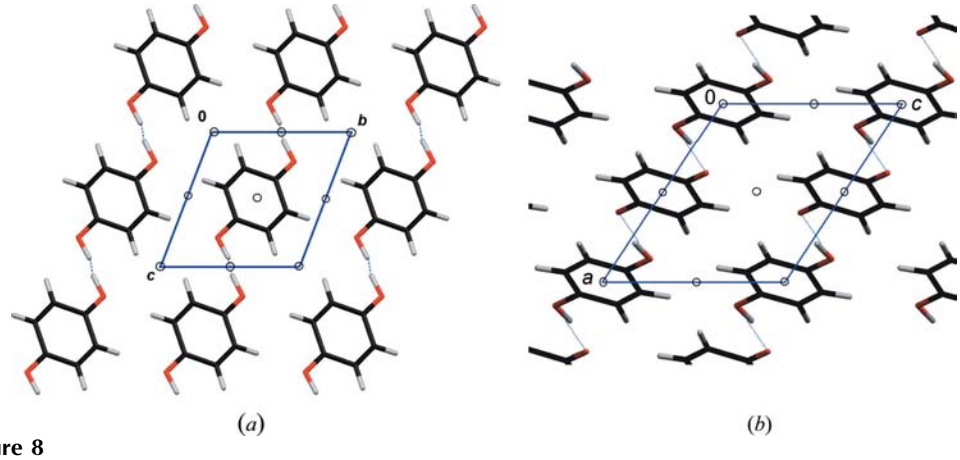

Figure 8
Crystal packing of (*a*) the triclinic polymorph of *p*-benzosemiquinone and (*b*) the triclinic polymorph of quinhydrone viewed normal to the *ac* plane with symmetry elements shown. In the triclinic *p*-benzosemiquinone, the disordered H1 proton is drawn in symmetry-equivalent positions to emphasize the symmetry of the hydrogen bond, whereas the population of each site is 0.5.

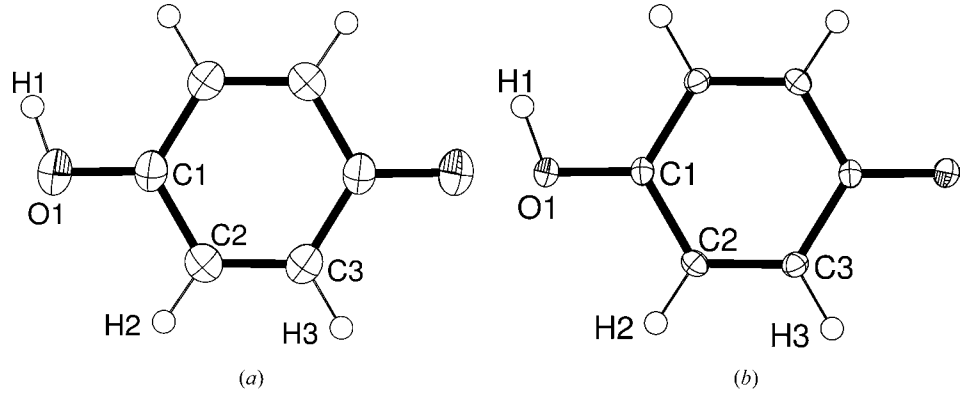

Figure 9
Molecular structure of the *p*-benzosemiquinone radical of the triclinic polymorph of *p*-benzosemiquinone obtained from data recorded at (*a*) room temperature and (*b*) 90 K. The atoms of an asymmetric unit are labelled.

Table 4
Hydrogen bond length O1—H1···O1 as a function of temperature for the monoclinic polymorph of semiquinone.

	Temperature				
	90 K	150 K	200 K	250 K	298 K
O1—H1···O1 (Å)	2.709 (3)	2.707 (4)	2.724 (3)	2.731 (2)	2.744 (2)

bonded to the O atom, apparently does not interact with the unpaired electron. The lack of interaction can be explained by resonance and the formation of a low-barrier hydrogen bond, as discussed in §3.5.

3.5. Proton disorder and the low-barrier hydrogen bond

To shed more light on the role of the O1—H1···O1 hydrogen bond on the stabilization of the *p*-benzosemiquinone radical, variable-temperature X-ray diffraction was used.

The bond lengths of the O1—H1···O1 hydrogen bond observed in both polymorphs, monoclinic and triclinic, at different temperatures are shown in Table 4. The hydrogen bond of 2.74 Å observed at room temperature can be considered to be medium to strong and proton transfer should not be expected.

The symmetry of the O1—H1···O1 hydrogen bond, which is located on the crystallographic inversion centre, requires two positions of the H1 proton, with s.o.f. = 0.5; a case which is typical of static disorder. Owing to the bond length, two separate peaks should be expected in the case of static disorder. The difference-Fourier map (Fig. 11), however, reveals a single, broad maximum, *ca* 0.8 Å long. Its shape does not depend on the temperature, indicating a single, but broad potential well, like that shown in Fig. 3(*b*). It is unlikely that the maximum in Fig. 11 is a result of the overlapping electron density of two statically disordered proton positions, because of the large distance between them (*ca* 0.8 Å).

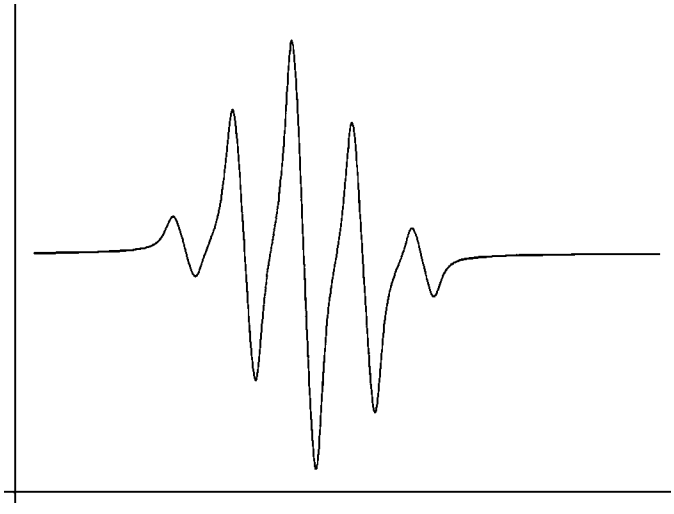

Figure 10
The EPR spectrum of the *p*-benzosemiquinone radical in the solid state.

Crystallographic data alone are insufficient to unambiguously distinguish between the static and dynamic disorder, however, the four-electron EPR spectrum (Fig. 10) supports the dynamic model. Placed in a potential well such as that in Fig. 3(*b*), the H1 proton would be fully delocalized and would not interact with electrons from the benzenoid rings. Its distribution function would then resemble the broad peak in the Fourier density map (Fig. 11). The statically disordered H1 proton, however, would be covalently bound to one of the O1 atoms and the EPR spectrum of such a crystal would indicate five protons, four of them being equivalent.

Our findings, therefore, although not definite, support the delocalized model and the potential well shown in Fig. 3(*b*).

4. Conclusion

We have described the crystal structures of two polymorphs of *p*-benzosemiquinone, the smallest organic radical crystallized so far. These structures are related to quinhydrone polymorphs, to which they can be converted by a single-crystal-to-single-crystal reaction. The radical molecules are stabilized by low-barrier hydrogen bonds, the longest of this type (2.74 Å) at room temperature.

The authors are indebted to Professor Dubravka Matković-Čalogović and Dalibor Milić of the Laboratory of General and Inorganic Chemistry, Faculty of Science, University of Zagreb, for data collection using an Oxford Diffraction diffractometer. Thanks also go to Dr Snježana P. Kazazić, Rudjer Bošković Insitute, for valuable help with the discussion of DFT calculations and for performing some additional DFT calculations.

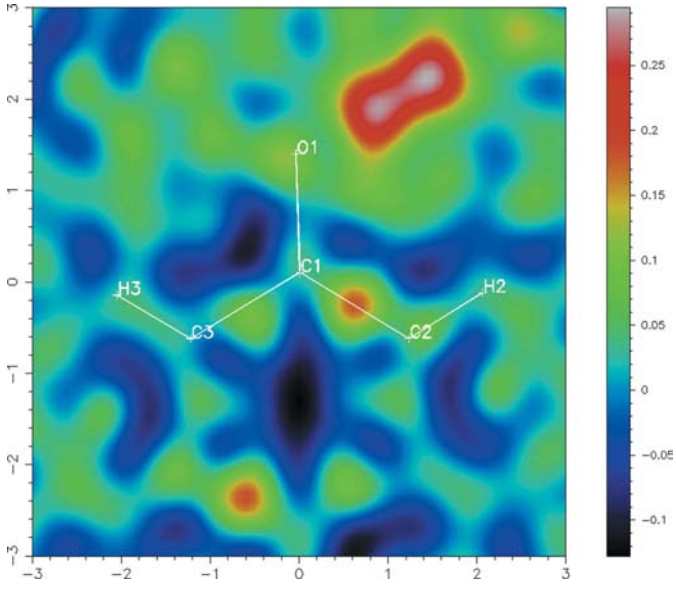

Figure 11
Difference Fourier maps of the monoclinic polymorph of *p*-benzosemiquinone at room temperature. An elongated positive peak (red area) near O1 corresponds to a delocalized H1 atom, suggesting a dynamical model. In the case of static disorder or tautomerism, two separated peaks would be expected. Separation distances are in Å and the colour-coded electron density is in e Å^{-3}.

The EPR spectrum was measured by PhD student Krunoslav Mirosavljević, Rudjer Bošković Institute, Zagreb, Croatia.

References

Artali, R., Marchini, N., Meneghetti, F., Cavazzini, D., Cassetta, A. & Sassone, C. (2005). *Acta Cryst.* D**61**, 481–484.

Asher, J. R., Doltsinis, N. L. & Kaupp, M. (2004). *J. Am. Chem. Soc.* **126**, 9854–9861.

Asher, J. R., Doltsinis, N. L. & Kaupp, M. (2005). *Magn. Reson. Chem.* **43**, S237–S247.

Banerjee, S. (1939). *Z. Kristallogr.* **100**, 316–355.

Berman, H. M., Westbrook, J., Feng, Z., Gilliland, G., Bhat, T. N., Weissig, H., Shindyalov, I. N. & Bourne, P. E. (2000). *Nucl. Acids Res.* **28**, 235–242.

Bolte, M. & Lerner, H.-W. (2001). Private Communication. CSD refcode HYQUIN06.

Bolte, M., Margraf, G. & Lerner, H.-W. (2002). Private Communication. CSD refcode BNZQUI03.

Breton, J. & Nabedryk, E. (1996). *Biochim. Biophys. Acta*, **1275**, 84–90.

Ciofini, I., Reviakine, R., Arbuznikov, A. & Kaupp, M. (2004). *Theor. Chem. Acc.* **111**, 132–140.

Cleland, W. W. (2000). *Arch. Biochem. Biophys.* **382**, 1–5.

Cowan, J. A., Howard, J. A. K., McIntyre, G. J., Lo, S. M.-F. & Williams, I. D. (2003). *Acta Cryst.* B**59**, 794–801.

Cowan, J. A., Howard, J. A. K., McIntyre, G. J., Lo, S. M.-F. & Williams, I. D. (2005). *Acta Cryst.* B**61**, 724–730.

Dikanov, S. A., Samoilova, R. J., Kolling, D. R. J. Holland, J. T. & Croftsl, A. R. (2004). *J. Biol. Chem.* **279**, 15814–15823.

Eggins, B. R. & Chambers, J. Q. (1970). *J. Electrochem. Soc.* **117**, 186–192.

Enraf–Nonius (1994). *CAD*-4 *Express Software*. Enraf–Nonius, Delft, The Netherlands.

Faig, M., Bianchet, M. A., Talalay, P., Chen, S., Winski, S., Ross, D. & Amzel, L. M. (2000). *Proc. Natl. Acad. Sci. USA*, **97**, 3177–3182.

Farrugia, L. J. (1997). *J. Appl. Cryst.* **30**, 565.

Farrugia, L. J. (1999). *J. Appl. Cryst.* **32**, 837–838.

Foz, O. R. & Palacios, J. (1932). *An. Soc. Esp. Fis. Quim.* **30**, 421–425.

Gomez, P. C. & Pacios, L. F. (2005). *Phys. Chem. Chem. Phys.* **7**, 1374–1381.

Guo, Q., Corbett, J. T., Yue, G., Fann, Y. C., Qian, S. Y., Tomer, K. B. & Mason, R. P. (2002). *J. Biol. Chem.* **277**, 6104–6110.

Harms, K. & Wocadlo, S. (1995). *XCAD*-4. University of Marburg, Germany.

Kaupp, M. (2002). *Biochemistry*, **41**, 2895–2900.

Kolling, D. R. J., Samoilova, R. I., Holland, J. T., Berry, E. A., Dikanov, S. A. & Crofts, A. R. (2003). *J. Biol. Chem.* **278**, 39747–39754.

Kumar, G. A., Pan, Y., Smallwood, C. J. & McAllister, M. A. (1998). *J. Comput. Chem.* **19**, 1345–1352.

Li, R., Bianchet, M. A., Talalay, P. & Amzel, L. M. (1995). *Proc. Natl. Acad. Sci. USA*, **92**, 8846–8850.

Matsuda, H., Osaki, K. & Nitta, I. (1958). *Bull. Chem. Soc. Jpn*, **31**, 611–620.

Mattar, S. M., Stephens, A. D. & Emwas, A. H. (2002). *Chem. Phys. Lett.* **352**, 39–47.

Mezzeti, A. & Liebl, W. (2005). *Eur. Biophys. J.* **34**, 921–936.

Mitani, T., Saito, G. & Urayama, H. (1988). *Phys. Rev. Lett.* **60**, 2299–2302.

Mohandas, P. & Umapathy, S. (1997). *J. Phys. Chem. A*, **101**, 4449–4459.

Nakasuji, K., Sugura, K., Kitagawa, T., Toyoda, J., Okamoto, H., Okaniwa, K., Mitani, T., Yamamoto, H., Murata, I., Kawamoto, A. & Tanaka, J. (1991). *J. Am. Chem. Soc.* **113**, 1862–1864.

Nonella, M. (1997). *J. Phys. Chem. B*, **101**, 1235–1246.

Nygren, C. A., Wilson, C. C. & Turner, J. F. C. (2005). *J. Phys. Chem. A*, **109**, 1911–1919.

O'Malley, P. J. & Collins, S. J. (1996). *Chem. Phys. Lett.* **259**, 296–300.

O'Malley, P. J. (1997). *J. Phys. Chem. A*, **101**, 6334–6338.

O'Malley, P. J. (1998). *Chem. Phys. Lett.* **291**, 367–374.

Palacios, J. & Foz, O. R. (1935). *An. Soc. Esp. Fis. Quim.* **33**, 627–642.

Palacios, J. & Foz, O. R. (1936). *An. Soc. Esp. Fis. Quim.* **34**, 779–781.

Parkin, A., Harte, S. M., Goeta, A. E. & Wilson, C. C. (2004). *New J. Chem.* **28**, 718–721.

Perrin, C. L. & Nielson, J. B. (1997). *Ann. Rev. Phys. Chem.* **48**, 511–544.

Sakurai, T. (1965). *Acta Cryst.* **19**, 320–330.

Sakurai, T. (1968). *Acta Cryst.* B**24**, 403–412.

Sheldrick, G. M. (1997*a*). *SHELXS*97. University of Göttingen, Germany.

Sheldrick, G. M. (1997*b*). *SHELXL*97. University of Göttingen, Germany.

Shigeta, Y., Kitagawa, Y., Nagao, H., Yoshioka, Y., Toyoda, Y., Nakasuji, K. & Yamaguchi, K. (2001). *J. Mol. Liquids*, **90**, 69–74.

Sinnecker, S., Reijerse, E., Neese, F. & Lubitz, W. (2004). *J. Am. Chem. Soc.* **126**, 3280–3290.

Steiner, T., Majerz, I. & Wilson, C. C. (2001). *Angew. Chem. Int. Ed.* **40**, 2651–2654.

Stowell, M. H. B., McPhillips, T. M., Rees, D. C., Soltis, S. M., Abresch, E. & Feher, G. (1997). *Science*, **276**, 812–816.

Tuckerman, M. E., Marx, D., Klein, M. L. & Parinello, M. (1997). *Science*, **275**, 817–820.

Uchida, Y., Okabe, C., Kishi, A., Takeshita, H., Suzuki, Y., Nibu, Y., Shimada, R. & Shimada, H. (2002). *Bull. Chem. Soc. Jpn*, **75**, 695–703.

Venkataraman, B. & Fraenkel, G. K. (1955). *J. Chem. Phys.* **24**, 588–589.

Venkataraman, B., Segal, B. G. & Fraenkel, G. K. (1959). *J. Chem. Phys.* **30**, 1006–1016.

Vishweshwar, P., Jagadeesh Babu, N., Nangia, A., Mason, S. A., Puschmann, H., Mondal, R. & Howard, J. A. K. (2004). *J. Phys. Chem. A*, **108**, 9406–9416.

Wilson, C. C. (2001). *Acta Cryst.* B**57**, 435–439.

Wilson, C. C. & Goeta, A. E. (2004). *Angew. Chem. Int. Ed.* **43**, 2095–2099.

Wilson, C. C., Shankland, K. & Shankland, N. (2001). *Z. Kristallogr.* **216**, 303–306.